SUPPORTING INFORMATION:

Molecular basis for specific viral RNA recognition and 2'-*O* ribose methylation by the dengue virus NS5 protein

Supporting Text; Supporting Figures; Supporting Tables

Supporting Text (Materials and Methods)

Cells. For transfection, BHK-21 cells (Baby Hamster Kidney fibroblast cells) were maintained in DMEM media (Gibco), supplemented with 10% fetal bovine serum (FBS) and 1% penicillin/streptomycin (P/S) at 37°C in 5% CO_2. For plaque assay, BHK-21 cells were maintained in RPMI 1640 media (Gibco), supplemented with 10% FBS and 1% P/S at 37°C in 5% CO_2.

Construction of mutant DENV2 full-length infectious clone. DENV2 full-length cDNA clones with NS5 E111A, E111Q and E111R mutations were constructed with a pACYC-NGC FL and a TA-NGC (shuttle E) vector as previously described (1). The pACYC-NGC FL plasmid contains a long DNA fragment comprising a T7 promoter, the DENV2 NGC genome, and the hepatitis delta virus ribozyme sequence (HDVr). The shuttle vector contains nucleotides 5427 to 10955 (from NS3 to 3'UTR and HDVr sequence) from the pACYC-NGC FL plasmid. All mutations were engineered into the shuttle E vector, using QuikChange II XL site-directed mutagenesis kit (Stratagene) according to the manufacturer's protocol. The primers used for site directed mutagenesis are listed in **Table S3A**. The mutants were cloned into pACYC-NGC FL at *BspEI* and *MluI* restriction sites. All constructs were verified by DNA sequencing before proceeding to the subsequent experiments.

DENV2 full-length cDNA clones with substitutions at the position of 5' nucleotide G_2 were engineered by PCR using Phusion DNA Polymerase under standard procedures. The primers used for introducing 5' UTR mutations are listed in **Table S3B**. The PCR products were purified and checked by DNA sequencing before cloning into pACYC-NGC FL at *NotI* and *NheI* restriction sites.

***In vitro* transcription and RNA transfection.** The full-length wild-type and mutants DENV2 infectious cDNA clones were linearized with *XbaI* and purified with phenol-chloroform. The purified linearized cDNAs were then subjected to *in vitro* transcription using T7 mMESSAGE mMACHINE kit according to the manufacturer's protocol (Ambion, U.S.A.). Approximately 10 µg *in vitro* transcribed RNAs was mixed with 8×10^6 BHK-21 cells in 0.8 ml Ingenio Electroporation Solution (Mirus) in a pre-chilled 0.4 cm cuvette, and electroporated at settings of 850 V and 25 µF, 3 pulses at 5-10 sec intervals. After a 10-min recovery at room temperature, the transfected cells were resuspended in 25 ml pre-warmed DMEM containing 10% FBS.

Plaque assay. Virus stock was produced by harvesting the supernatant of DENV2 full-length RNA-transfected BHK-21 cells at 24, 48, 72, 96, and 120 hours post transfection. Virus titer and morphology were determined by standard plaque assay. Briefly, a series of 10-fold dilutions was prepared by first diluting 50 µl virus stock with 450 µl RPMI 1640 media containing 2% FBS to obtain 10^{-1} dilution and then further diluted until a final 10^{-6} dilution was achieved. Confluent BHK-21 cells (1×10^5 cells per well, plated 2 days in advance) grown in 24-well plate was added with 200 µl of each dilution per well. Duplicates were prepared for each time point and dilution factor. The infection was allowed to proceed at 30°C for 1 hour, followed by removing the media and adding 500 µl 0.8% methyl-cellulose overlay (containing RPMI, 2% FBS, 1% P/S, 0.05% $NaHCO_3$, 25 mM Na Hepes, and 0.5% DMSO) into each well. The plates were incubated for 5 days at 37°C in 5% CO_2 before fixing in 3.7% formaldehyde and staining with 1% crystal violet. The viral titer was calculated as plaque-forming unit (PFU) per ml.

Viral RNA extraction and quantification. For intracellular viral RNA quantification, DENV2 full-length RNA-transfected BHK-21 cells were seeded into 6-well plate at 3.2×10^5 cells per well and incubated at 37°C in 5% CO_2. At 24 h post transfection (hpt), the media was changed to DMEM containing 2% FBS and the plate was incubated at 30°C in 5% CO_2. At indicated time points (6, 24, 48, 72, 96, and 120 hpt), the cells were washed once with PBS before lysing with TRIzol reagent (Invitrogen). RNA extraction was carried out according to the manufacturer's instructions. To quantify total intracellular viral RNA, a quantity of 100 ng of extracted RNA was subjected to real time RT-PCR using a Bio-Rad CFX96 real-time PCR detection system, through the use of iScript enzyme one-step RT PCR with SYBR and primers (forward, 5'-CGTCGAGAGAAATATGGTCACACC-3'; and reverse, 5'-CCACAATAGTATGACCAGCCT-3') targeting the DENV2 NS5 methyltransferase (MTase) region. A plasmid fragment containing genome sequences of the DENV2 NS5 MTase region generated from DENV2 WT IVT RNA was used to establish a standard curve for quantification of viral genome copy number. For extracellular viral RNA quantification, supernatant of DENV2 full-length RNA-transfected BHK-21 cells was harvested at 24, 48, 72, 96, and 120 hpt, and clarified before adding TRIzol LS reagent (Invitrogen). RNA extraction was carried out following the manufacturer's instructions and the extracted RNA was subjected to real time RT-PCR as described above. The extracted RNA at 24 and 120 hpt were also used for RT-PCR by using a series of overlapping primers

covering the whole NS5 gene of DENV2. The RT-PCR products were then purified with gel extraction kit and sent for DNA sequencing.

Expression and purification of DENV4 WT and mutant MTase proteins. The R38A, K42A, R57A, R84A, E111A, E111Q, E111R, R212A, S214A and T215A mutations in the DENV4 NS5 sequence were engineered into the plasmid pGEX-4T-1+D4(MY22713)+SAM272, using QuikChange II XL SDM kit according to the manufacturer's protocol (Stratagene). The primers used for site directed mutagenesis are listed in **Table S3C**. The plasmid contains DENV4 genome sequence encoding amino acids 1 to 272 of the NS5 MTase protein. All constructs were verified by DNA sequencing before proceeding to protein expression and purification. Expression plasmids for all recombinant MTase proteins fused with a N-terminal GST-tag were transformed into BL21 competent cells, and grown on LB plate containing ampicillin at 37°C. Colonies were scraped and inoculated into 2 ×YT medium containing ampicillin at 37°C with shaking at 180 rpm until an absorbance optical density at 600 nm of 0.6 to 0.8 was reached. Protein expression was induced overnight with 0.4 mM isopropyl-β-D-thiogalactopyranoside (IPTG) at 16°C. After overnight incubation, cells were harvested and cell pellet was sonicated in buffer A (20 mM Tris-HCl at pH 7.5, 0.5 M NaCl, 2 mM β-mercapto-ethanol, 5% glycerol) supplemented with 0.01% 3-[(3-Cholamidopropyl)dimethylammonio]-1-propanesulfonate (CHAPS) and protease inhibitor cocktail tablet (Roche). The cell supernatant was filtered and loaded on a GSTrap™ FF column (GE Healthcare) pre-equilibrated with buffer A. The GST-tag was cleaved overnight at 4°C using thrombin, and DENV4 MTase was purified through the GSTrap™ FF and HiTrap™ Benzamidine FF columns (GE Healthcare). The protein was further concentrated and stored at -80°C before use. Protein stability was analyzed by thermo-fluorescence assay as described previously (2).

Construction of mutant $^{m7}G_{0ppp}$-DENV4 5'UTR nt-110 RNAs for 2'-*O* MTase assay. DENV4 5'UTR nt-110 DNA with substitutions at the position of 5' nucleotide G_2 was engineered by PCR using Phusion DNA Polymerase under standard procedures. The primers used for introducing 5' UTR mutations are listed in **Table S3D**. The PCR products were purified and checked by DNA sequencing before subjecting to *in vitro* transcription (IVT) using MEGAshortscript T7 Transcription Kit (Life Technologies). ^{m7}GpppA cap analog was added in the transcription reaction to obtain RNA containing the cap structure. The IVT RNAs were then purified and resuspended in RNase-free water.

DENV4 2'-*O* MTase assay. DENV4 2'-*O* MTase assay was performed as described previously (3, 4). The 2'-*O* MTase reaction comprised 25 nM protein, 40 nM biotinylated $^{m7}G_{0ppp}$-DENV4 5'UTR nt-110 RNA and 320 nM [^{3}H-methyl]-SAM in 50 mM Tris-HCl at pH 7.5, 10 mM KCl, 2 mM $MgCl_2$, and 0.05% CHAPS. Buffer, RNA substrate, and enzyme were first mixed in a single well in a 96-well half-area, white opaque plate (Corning Costar, Acton, MA), and the reaction was initiated by addition of [^{3}H-methyl]-SAM and incubation at RT for 1 hr. After incubation, the reaction was stopped with an equal volume of 2 × stop solution (100 mM Tris HCl at pH 7, 50 mM EDTA, 300 mM NaCl, 4 mg/ml streptavidin-SPA beads, and 62.5 μM cold SAM). The plate was shaken for 20 min at 750 rpm at room temperature followed by centrifugation for 2 min at 1200 rpm and read in a TriLux MicroBeta counter (PerkinElmer, Boston, MA) with a counting time of 1 min/well. All data points were collected in duplicate wells.

DENV4 NS5 polymerase *in vitro* assays. The *de novo* initiation/elongation assay was performed similarly as described earlier (2). Briefly, the reaction comprised 100 nM DENV4 NS5, 100 nM in vitro transcribed DENV4 5´UTR-3´UTR RNA, 20 μM ATP, 20 μM GTP, 20 μM UTP, 5 μM Atto-CTP (Trilink Biotechnologies), in a volume of 15 μl of the assay buffer comprising 50 mM Tris-HCl, pH 7.5, 10 mM KCl, 1 mM $MgCl_2$, 0.3 mM $MnCl_2$, 0.001% Triton X-100 and 10 μM cysteine. The elongation assay reaction comprised 100 nM IVT 244 nt heteropolymeric RNA template, annealed with four primers (C1 primer 3'-AGTCAGTCAGTCAGTGT- 5', A1 primer 3'-GTCAGTCAGTCAGTCTC- 5', G1 primer 3'-TCAGTCAGTCAGTCACA- 5', T1 primer 3'-CAGTCAGTCAGTCAGAG-5')(5), 2 μM ATP, 2 μM GTP, 2 μM UTP, 0.5 μM Atto-CTP, and 100 nM of DENV4 NS5 in 15 μl in assay buffer comprising 50 mM Tris-HCl at pH 7.5, 10 mM KCl, 0.5 mM $MnCl_2$, 0.01% Triton X-100, and 10 μM cysteine. RNA was separately pre-annealed to the four different sets of primers at a ratio of 1:2 (w/w) by heating at 95°C for 3 min, and cooled to RT before mixing and used for the assay. All reactions were allowed to proceed for up to 3 hrs at RT. At the indicated time-points, 10 μl of 2.5× STOP buffer (200 mM NaCl, 25 mM $MgCl_2$, 1.5 M DEA, pH 10; Promega) with 25 nM calf intestinal alkaline phosphatase (CIP; New England Biolabs) was added to the wells to terminate the reactions. The plate was shaken and centrifuged briefly at 1200 rpm, followed by incubation at RT for 60 min and the released AttoPhos was monitored by reading on a Tecan Saffire II microplate reader at excitation max and emission max wavelengths of 422 nm and 566 nm respectively. All data points were collected in triplicate wells in 384-well black opaque plates (Corning).

Thermo-denaturation fluorescence assay. Thermo-denaturation fluorescence analysis of proteins binding to cap0-7mer-RNA was performed similarly as described previously (2, 3). Briefly, 2.5 µM protein, with or without 50 µM 5'-$^{m7}G_{ppp}$AGUUGUU-3' RNA (Trilink) and SYPRO Orange dye (Invitrogen) in 1x assay buffer (50 mM Tris-Cl at pH 7.5, 100 mM KCl, 0.001% Triton X-100, 0.1 mM $MnCl_2$ and 0.1 mM $MgCl_2$) were mixed in a white opaque 96-well PCR plate (Bio-Rad), sealed and heated from 25°C to 85°C with increments of 0.5°C using CFX96 Touch Real-Time PCR Detection System (Bio-Rad). The excitation and emission wavelengths were 485 nm and 625 nm, respectively. Each experiment was done with duplicate wells and the rate of the change in fluorescence (-dRFU/dT) was plotted over temperature where RFU denotes relative fluorescence units and T represents time in seconds.

Crystallization and data collection. Crystallization was set-up at 20 °C using the hanging drop vapour diffusion and published conditions (6). Native crystals obtained over 2–5 days by mixing a volume of 1 µl of NS5 (6-895) at 4-6 mg/ml with 1 µl of precipitation solution (0.2 M magnesium acetate, 0.1 M sodium cacodylate, pH=6.4, 10-20% (w/v) PEG 8000) were soaked with 1mM of $^{m7}G_{0ppp}A_1G_2U_3U_4G_5U_6U_7$-3' overnight. Prior to data collection, crystals were soaked for a few seconds in a cryoprotecting solution containing 20% (v/v) glycerol before being mounted and cooled to 100 K in liquid nitrogen. Diffraction intensities were collected at the PXIII (X10SA) beamline of the Swiss Light Source, Paul Scherrer Institut, Villigen, Switzerland. Integration, scaling, and merging of the intensities were carried out using programs MOSFLM and SCALA from the CCP4 suite (7). The asymmetric unit contains one NS5 molecule with S-adenosyl-L-homocysteine (SAH) (copurified from *E. coli*) and RNA bound to the MTase domain. Crystal parameters and data collection statistics are summarized in **Table 1**.

Structure solution and refinement. The crystals have a solvent content of 50.2% and a Matthews coefficient (Vm) of 2.47 (8). Refinement was initiated with structure 4V0Q using REFMAC5 (9) and PHENIX (10) and interspersed with manual model rebuilding sessions using Coot (11). TLS refinement was introduced in the last refinement steps. The quality of the structure was analyzed using Molprobity (12). A summary of structure refinement statistics is given in **Table 1**. Superimpositions of structures were carried out using the program LSQKAB from the CCP4 suite. Figures were prepared using the program Pymol (13). The structure of NS5 with RNA and SAH bound to the MTase domain is very similar to the NS5: SAH structure (4V0Q) and the NS5:SAH:GTP structure (4V0R): The root mean square deviation (r.m.s.d.) is 0.27 Å for a total of 739 Cα atoms superimposed. The refined coordinates were deposited in the PDB under accession code 5DTO.

Supporting Figures

Figure S1. Stereo views of the electron density maps for the bound RNA and SAH. (**a)** Simulated annealing $mF_{obs} - DF_{calc}$ omit maps (where the RNA, Mg^{2+} and SAH ligands were omitted from phase calculation) are colored in green and contoured at 3σ. (**b**) Magnified view of panel (**a)**. **(c)** $2mF_{obs} - DF_{calc}$ maps after refinement are colored in blue and contoured at 1σ. RNA Mg^{2+} ion in green and the surrounding water molecules in red are shown as spheres. RNA and SAH are shown in sticks.

a

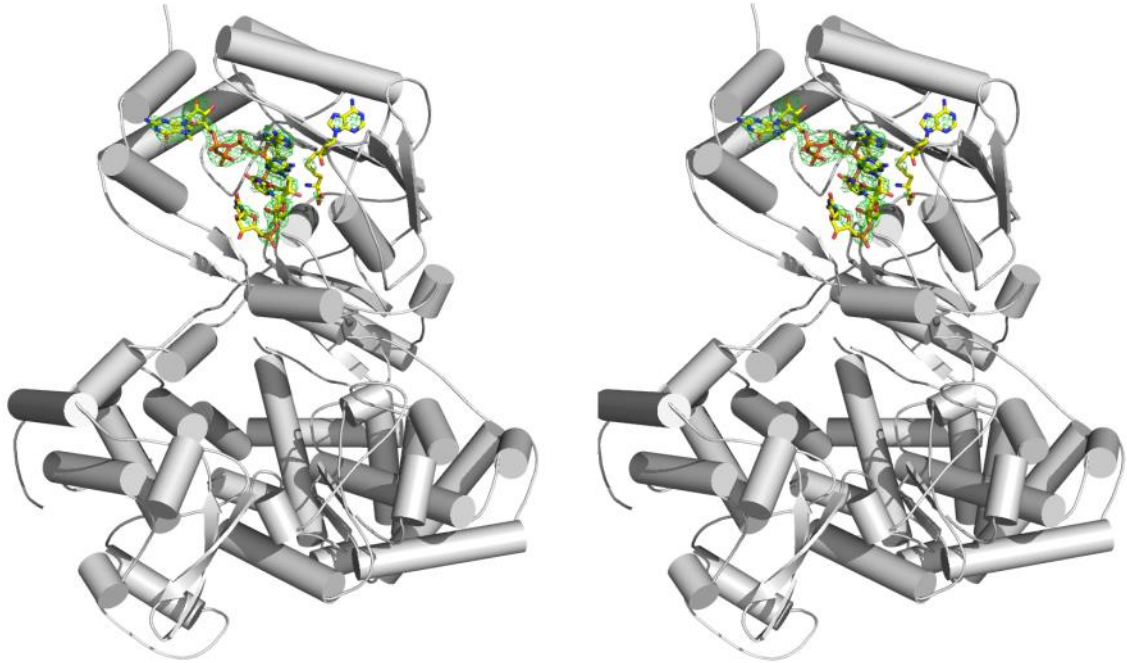

b

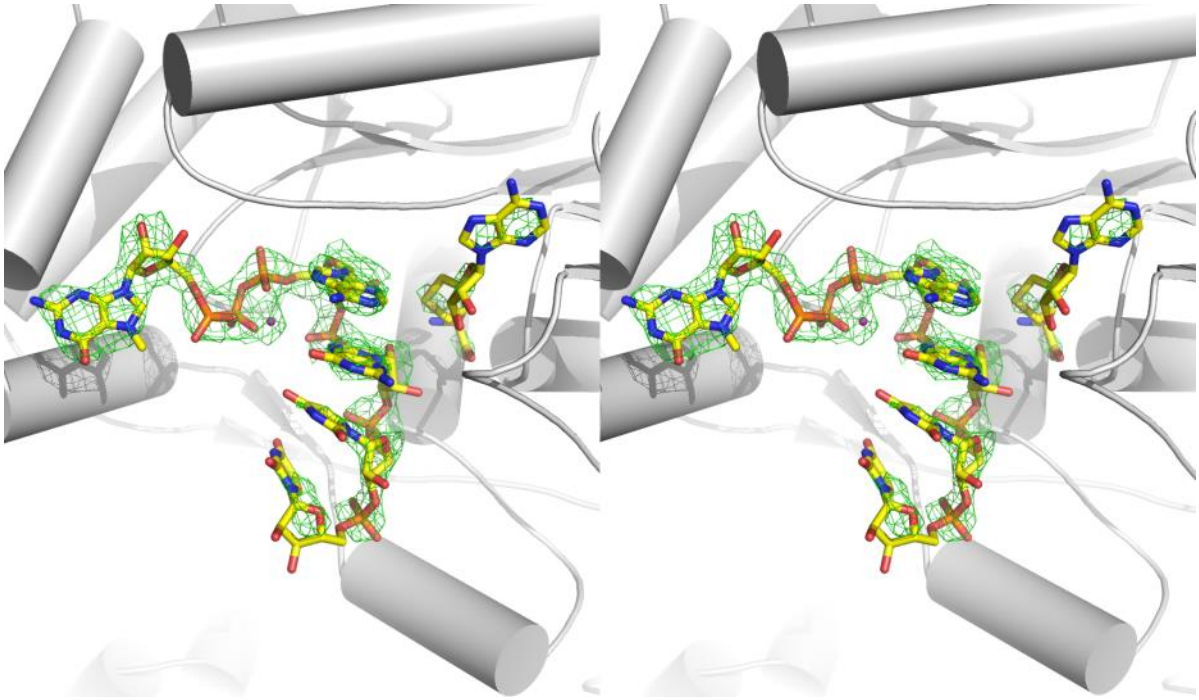

c

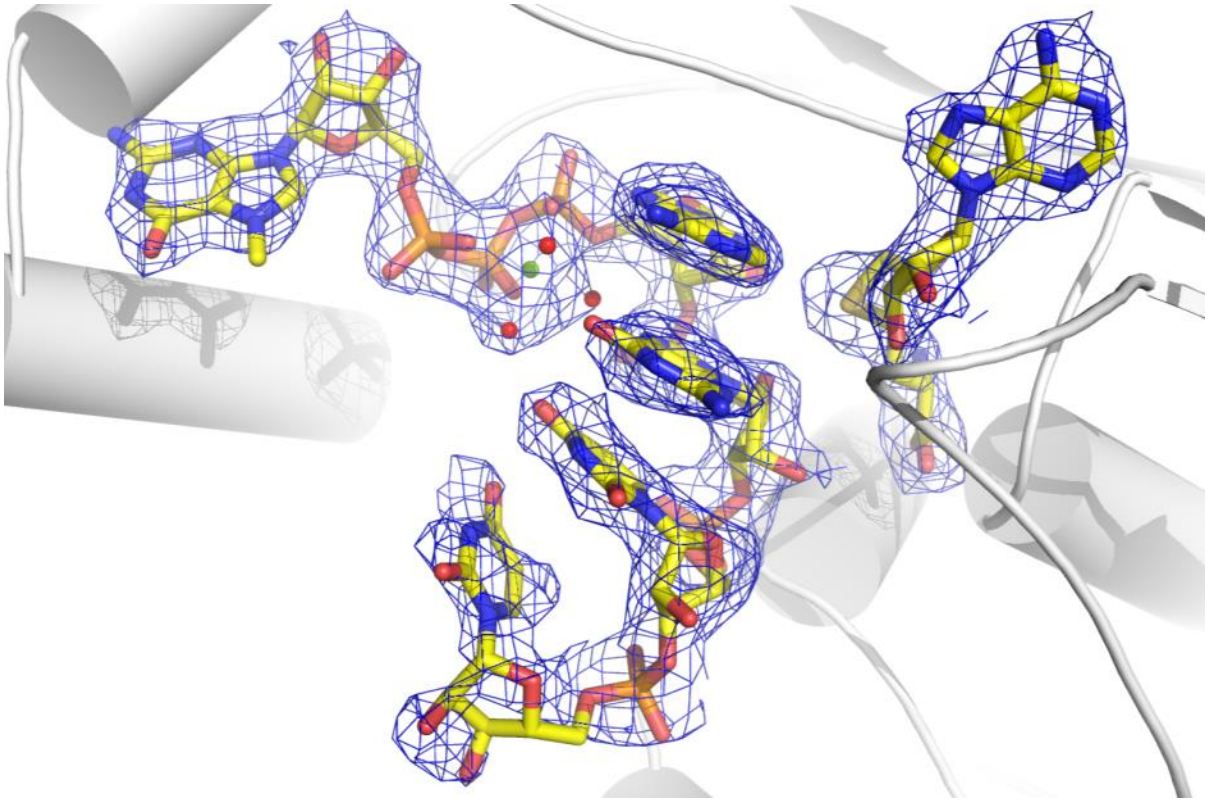

Figure S2: Local protein environment selects adenine as the first base and favours guanine as the second base. (**a)**. Modelling of RNA X_1= G, U or C ($^{m7}G_{0ppp}X_1$-RNA) ($^{m7}G_{0ppp}X_1$-RNA) in place of A_1: N2 amine group from G_1 collides with the ribose ring of the SAH moiety (closest distance ~ 1 Å) while a pyrimidine base would leave a large empty space in the pocket, leading to interactions energetically less favourable than with adenine. (**b)** Modelling of RNA X_2=A, U or C ($^{m7}G_{0ppp}AX_2$-RNA) in place of G_2: other bases are unable to form equivalent polar contacts with the carboxylic group from E_{111} of the NS5 MTase domain, and introduce unfavourable charge-charge repulsion. **(c)**. Multiple sequence alignment of the first 12-nucleotides from various flavivirus genomes. **(d)** Modelling NS5 protein carrying E_{111} to A, Q or R.

a

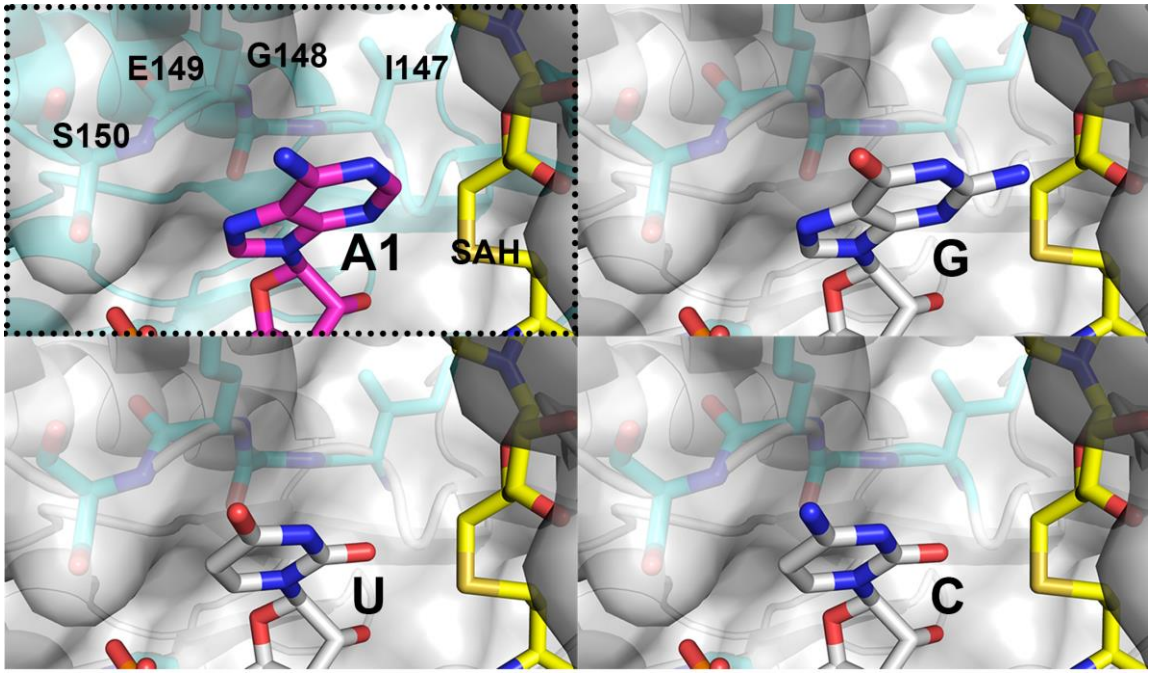

b

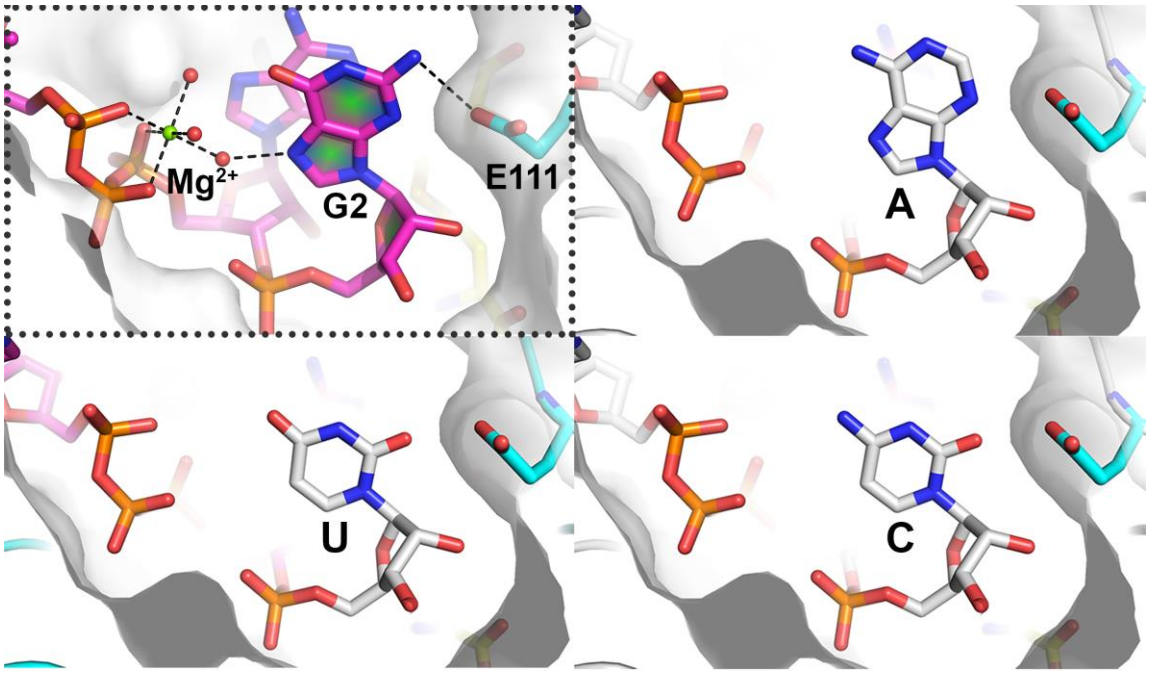

c

DENV1	**AG**UUGUUAGUCU
DENV2	**AG**UUGUUAGUCU
DENV3	**AG**UUGUUAGUCU
DENV4	**AG**UUGUUAGUCU
JEV	**AG**AAGUUUAUCU
WNV	**AG**UAGUUCGCCU
YFV	**AG**UAAAUCCUGU
TBEV	**AG**AUUUUCUUGC

d

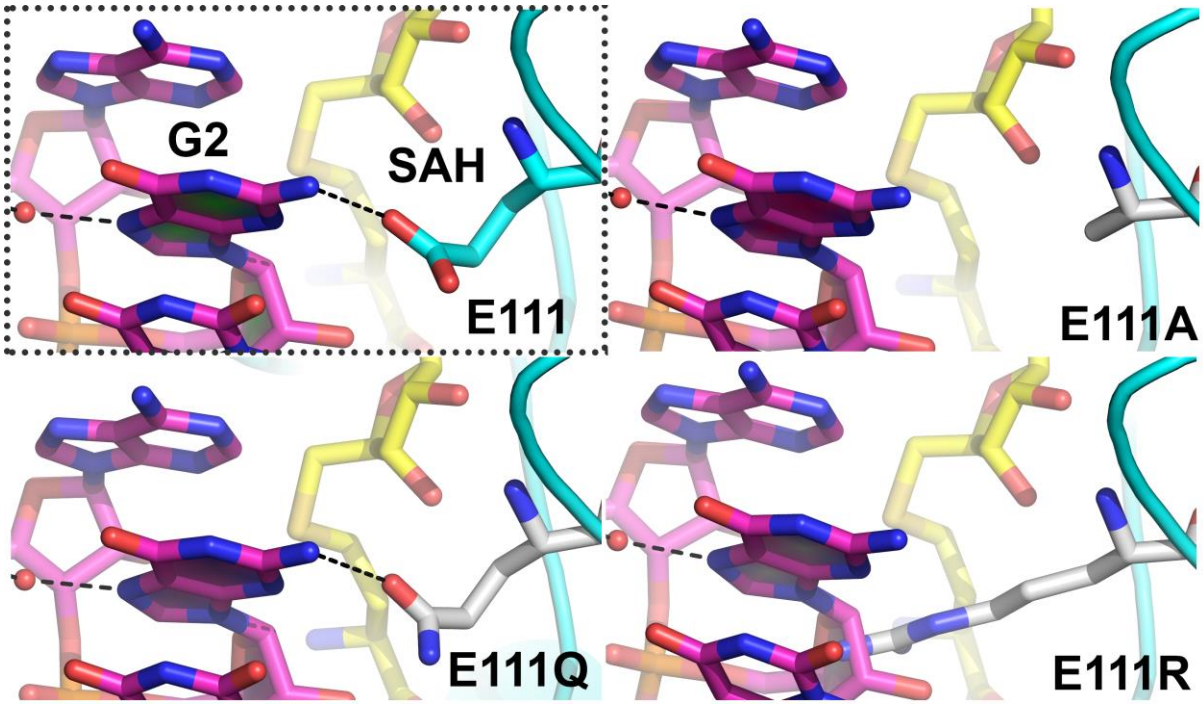

Figure S3. Enzymatic mechanism for viral RNA 2'-*O* methylation. (a) Stereochemistry of the NS5 MTase active site derived from the present ternary complex. Distances and angles between the NH2 group of the proposed activating general base K_{180}, the 2'-O of the adenosine A_1 adenosine ribose and the methyl group are indicated. The conformation of bound RNA brings the attacking nucleophile 2'-*O* atom of the A_1 adenosine ribose at a distance of 3.4 Å from the sulphur of SAH. The S_δ-CH3 methyl bond of the SAM methyl donor was modelled using the bound SAH structure (this work), giving a C_ε-O distance of 2.30 Å. This distance is intermediate between theoretical values of 2.96 Å and 1.97 Å that were calculated for the reactant and transition complex respectively (14). The S_δ-C_ε bond of SAM and the ribose 2'-O subtends an angle close to 180^o as expected for an in-line S_N2 attack for methyl transfer (15). **(b)** Superposition of the structure reported in this study (NS5 is coloured in cyan, RNA in magenta, SAH in yellow) and the DENV3 MTase domain in complex with a capped-RNA octamer (NS5 MTase in green, RNA in blue, SAH in yellow) (PDB code: 2XBM)(16). Only G0 is well aligned for the bound RNAs. K29, highly conserved across all flaviviruses, may serve as the catalytic residue for GTase, given its close distance to the alpha phosphate of G0.

a

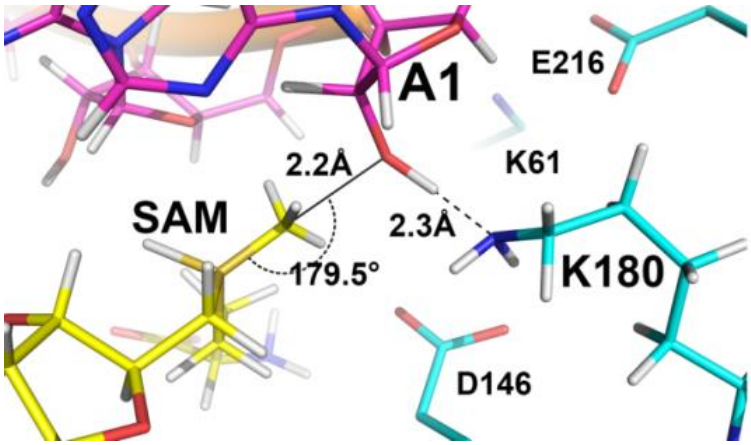

b

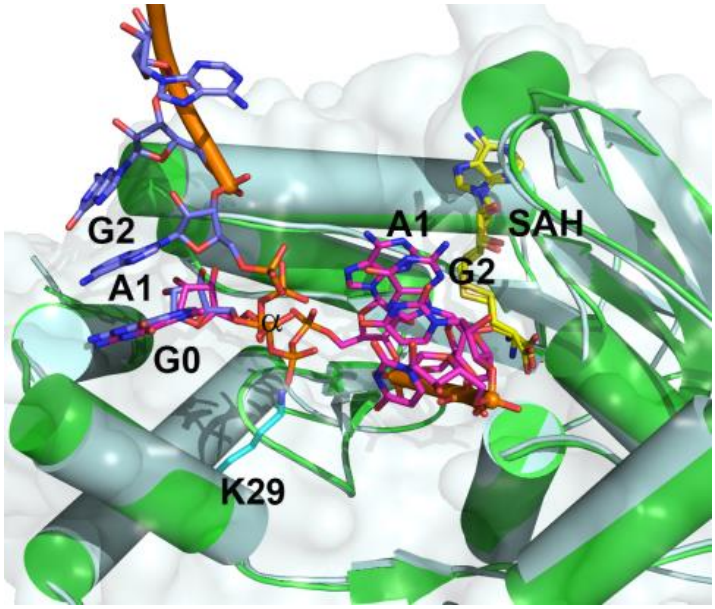

Figure S4. Structure based alignment of NS5 with non-flavivirus MTases. (**a**) Amino acid sequences alignment of the top 10 non-flavivirus hits with NS5 (from the Dali server, *www.ebi.ac.uk/Tools/structure/**dali**lite/*) and secondary structure assignments by program DSSP (*swift.cmbi.ru.nl/gv/**dssp**/).* The most frequent amino acid type is coloured in each column. The "KDKE" catalytic tetrad is highlighted in yellow. (**b**) Overall folds of the MTases from the hits. Proteins are shown as "cartoons" with the "KDKE" motif as sticks. RNA and SAH are shown as sticks with yellow carbons. (**c**) Close-up view of the MTase active sites from the hits.

a

b

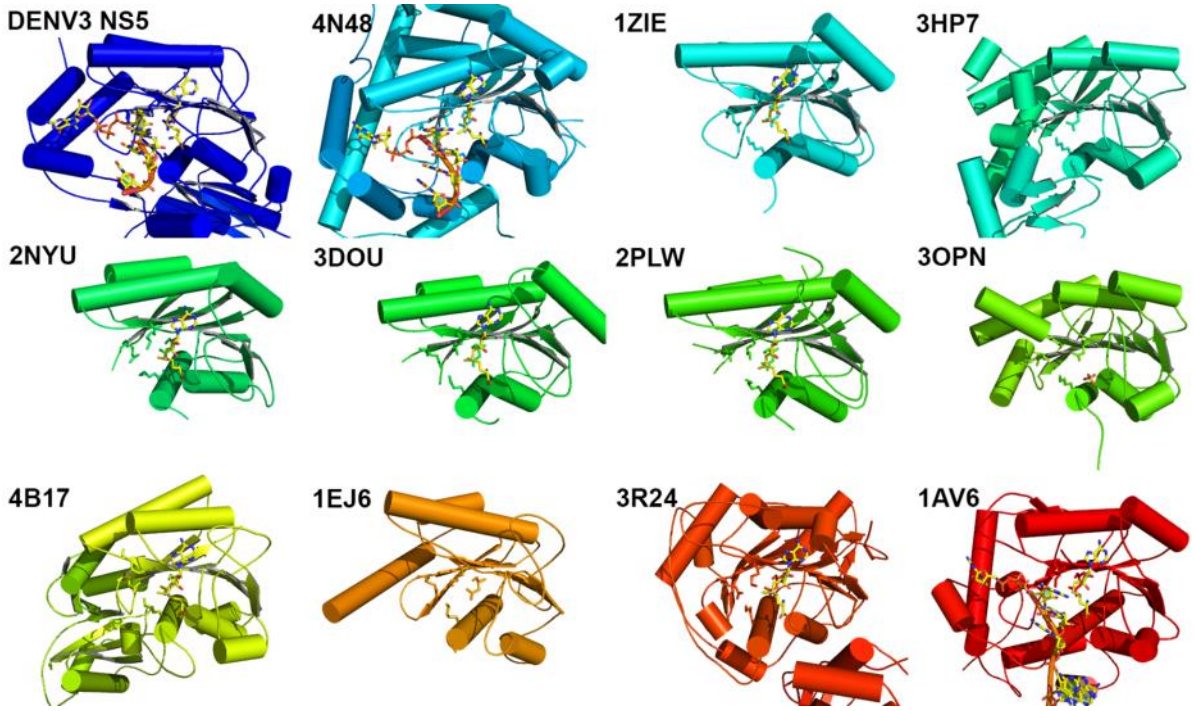
DENV3 NS5
4N48
1ZIE
3HP7
2NYU
3DOU
2PLW
3OPN
4B17
1EJ6
3R24
1AV6

c

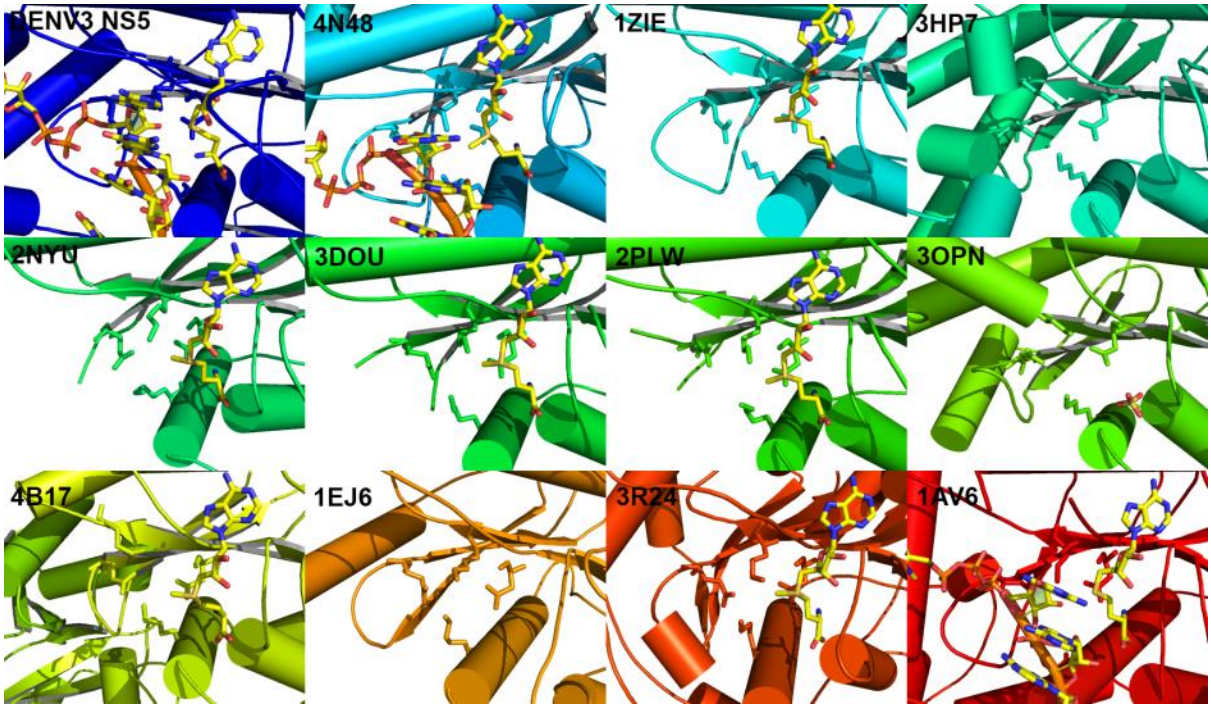
DENV3 NS5
4N48
1ZIE
3HP7
2NYU
3DOU
2PLW
3OPN
4B17
1EJ6
3R24
1AV6

Movie S1. Structure of the ternary complex between DENV3 NS5, capped RNA and SAH.

Supporting Tables

Table S1a: NS5 residues interacting with RNA or SAH and the effects of alanine mutations on 2'O-methyltransferase activities.

DENV3 NS5	**RNA atom/base**	**Distance** Å	**2'-O MTase activity**		**remarks**
			DENV4	**WNV**	
K14 NZ	G0 2'O	2.6	2 [a]	7[b]	
L17 O	G0 N2	3.1		41[b]	Main chain
N18 OD1	G0 2'O	3.0	70 [a]	52[b]	
L20 O	G0-N2	2.8			Main chain
F25	G0	Base stacking	4 [a]	33[b]	
K29 NZ	G0-O1A	> 4.0	15 [a]	46[b]	Long range electrostatic
R38 NH2	U4-OP1	>4.0	8.9*		
K42 NZ	U4-OP1	> 4.0	76.7*	90[b]	Long range electrostatic
R57 NH2	G2-OP1	2.4	8 [a]/0*	6[b]	
K61 NZ	A1-OP1	2.9	0 [a]	0[b]	KDKE motif
R84 NH1	U3-2'O	> 4.0	62 [a]/68.4*	100[b]	Long range electrostatic
E111 OE1	G2-N3	2.8	94 *	57[b]	
D146 OD2	A1-2'O	> 4.0	0 [a]	0[b]	KDKE motif
S150 N	A1-N7	3.3	55 [a]	62[b]	
K180 NZ	A1-2'O	2.3	6 [a]	0[b]	KDKE motif
R211 NH1	H2O/U3-OP2	3.4-2.2	29 [a]/2.7*	7[b]	R212
S213 OG	G0-O2B	2.6	94 [a]/79.2*		S214
T214 OG1	G0-O2C	3.4	79*/41.9*	104[b]	
E216 OE1	K61-NZ	2.6	0 [a]	0[b]	KDKE motif
Y218 OH	K61-NZ; D146-OD1	3.5; 2.8		8[b]	
DENV3 NS5	**SAH atom/base**	**Distance** Å	**DENV4**	**WNV**	
T104 OG1	H2O/ O2'	2.3-2.6			
K105 N	N3	3.0	61 [a]	70[b]	
H110 ND1	O2'	3.2	58 [a]	65[b]	
E111 OE1	O3'	3.5		57[b]	
D131 OD1	N6	2.8	13 [a]	3[b]	
V132 N	N1	3.1			
F133	Hydrophobic	-		92[b]	
D146 OD2	N	2.9	0 [a]	0[b]	KDKE motif
I147	Hydrophobic	-	15 [a]	5[b]	
K180 NZ	SD	4.7	6 [a]	0[b]	KDKE motif

[a]Dong et al., 2010, Virology Volume 405, (2), p568–578; [b] Dong et al., 2008, J. Virol., 82 (9) p4295–4307.*In this work.

Table S1b. *In vitro* 2'O MTase activities and thermo-stabilities of WT DENV4 MTase and E111 mutant proteins. SPA assay was performed with WT and mutant RNA templates as described in Materials and Methods. Results shown are the average percentage activity of mutant MTase proteins compared against WT protein. All data points and standard deviations are obtained from two independent experiments, each with duplicate measurements. Protein thermo-stability was determined from one experiment with duplicate measurements as described in Materials and Methods.

Percentage of WT and mutant MTase activity		DENV4 NS5 proteins			
		WT	E111A	E111Q	E111R
2'O MTase activities using DENV4 5'UTR G0-1-110nt RNA	G2 (WT)	100 ± 0	93.9 ± 1.7	93.4 ± 10.4	0
	A2	83.9 ± 5.2	62.4 ± 5.7	69.7 ± 3.0	4.0 ± 0.8
	U2	55.4 ± 1.4	37.1 ± 8.0	47.9 ± 12.3	2.4 ± 0.1
	C2	24.4 ± 4.7	26.8 ± 6.1	11.1 ± 0.3	0
Protein thermo-stability, Tm (°C)		39.5	39.0	39.0	38.5

Table S1c. *De novo* initiation/elongation activity and thermo-stability of DENV4 FL WT and E111 mutant NS5 proteins. Polymerase activities of DENV4 FL WT and mutant proteins were measured in *de novo* initiation/elongation and elongation FAPA assays. Results shown are the average percentage activity compared against WT protein derived from average relative fluorescence units (RFU) obtained for each protein from two independent experiments, each with triplicate measurements. Protein thermo-stabilities (Tm, protein melting temperature) with cap0-7mer-RNA were determined from two independent experiments, each with duplicate measurements, as described in Materials and Methods.

% NS5 activity	De novo Initiation/Elongation			Elongation			Thermo-fluorescence (°C)		
Time (hr)	1	2	3	1	2	3	Tm, no RNA	Tm, +RNA	ΔTm with RNA
WT	100 ± 0	100 ± 0	100 ± 0	100 ± 0	100 ± 0	100 ± 0	37.3 ± 0.3	41.0 ± 0	+3.7 ± 0.3
E111A	69.2 ± 5.2	67.9 ± 4.4	67.4 ± 10.3	30.9 ± 1.7	40.2 ± 5.4	38.5 ± 7.4	37.3 ± 0.3	38.5 ± 0	+1.2 ± 0.3
E111Q	116.5 ± 14.2	118.2 ± 21.8	119.7 ± 12.6	62.8 ± 0.8	71.5 ± 4.6	61.6 ± 7.0	36 ± 0	38.5 ± 0	+2.5 ± 0
E111R	92.8 ± 5.4	94.6 ± 2.8	101.2 ± 2.0	43.0 ± 0.9	51.3 ± 2.6	51.1 ± 1.3	35.5 ± 0	37.0 ± 0	+1.5 ± 0

Table S2: non-flaviviral NS5 MTase hits in PDB90, plus Mrna 2'O-ribose0MTase from SARS and Vaccinia viruses using DALI server (17). The 2nd to the 8th hits are also non-viral but ribosomal 2'-O-ribose RNA MTases from cellular organisms and two putative bacterial hemolysins (low sequence identity 14-20% and Z score 12.4-14.4). Following are the viral mRNA cap-specific 2'-O-ribose MTases: 9th - VP1 and 10th - λ2 proteins from Reoviruses - dsRNA viruses. NSP10/16 from SARS coronavirus - positive sense RNA virus - ranks at 19th and VP39 from Vaccinia virus - dsDNA virus - 42nd only.

NO:	PDB-CHAIN	Z	RMSD	LALI	NRES	%ID	SPECIES	DESCRIPTION
1:	4N48-B	16.2	2.9	222	406	14	HUMAN	CMTR1, CAP-SPECIFIC MRNA 2'-O-RIBOSE-METHYLTRANSFERASE (SMIETANSKI ET AL., 2014);
2:	1EIZ-A	14.4	2.4	155	180	19	ESCHERICHIA COLI	FTSJ, 23S RIBOSOMAL RNA METHYLTRANSFERASE (BUGL ET AL., 2000);
3:	3HP7-A	13.8	3.6	181	275	15	STREPTOCOCCUS THERMOPHILUS	STU1215, PUTATIVE HEMOLYSIN;
4:	2NYU-B	13.8	2.3	150	183	20	HUMAN	PUTATIVE RIBOSOMAL RNA METHYLTRANSFERASE 2;
5:	3DOU-A	13.6	2.2	148	176	18	THERMOPLASMA VOLCANIUM	RLME, RIBOSOMAL RNA LARGE SUBUNIT METHYLTRANSFERASE J;
6:	2PLW-A	13.2	2.2	146	183	14	PLASMODIUM FALCIPARUM	PF12_0052, PUTATIVE RIBOSOMAL RNA METHYLTRANSFERASE;
7:	3OPN-A	13.0	3.1	161	208	16	LACTOCOCCUS LACTIS	YIIB, PUTATIVE HEMOLYSIN;
8:	4B17-A	12.4	4.2	162	358	20	ESCHERICHIA COLI	RLMM, 23S RIBOSOMAL RNA 2'-O-RIBOSE-METHYLTRANSFERASE (PUNEKAR ET AL., 2012);
9:	3K1Q-A	12.2	3.3	189	1299	10	AQUAREOVIRUS	VP1, MRNA-CAPPING OUTER CAPSID PROTEIN (CHENG ET AL., 2010);
10:	1EJ6-A	11.2	3.4	199	1283	11	REOVIRUS	LAMBDA2, MRNA-CAPPING OUTER CAPSID PROTEIN (REINISCH ET AL., 2000);
19:	3R24-A	10.3	3.2	170	293	12	SARS CORONAVIRUS	NSP10/16, MRNA 2'-O-RIBOSE-METHYLTRANSFERASE (CHEN ET AL., 2011; DECROLY ET AL., 2011);
42:	1P39-A	9.6	3.8	178	292	13	VACCINIA VIRUS	VP39, CAP-SPECIFIC MRNA 2'-O-RIBOSE-METHYLTRANSFERASE (HODEL ET AL., 1998);

Table S3. List of DNA primers.

(A) Primers used for site-directed mutagenesis (SDM) of TA-NGC (shuttle E) plasmid

Mutation(s)[a]	Primer	
	Orientation[b]	**Sequence**
E111A	For	GAGGACCAGGACATGCAGAACCCATCCCCAT
	Rev	ATGGGGATGGGTTCTGCATGTCCTGGTCCTC
E111Q	For	AGGAGGACCAGGACATCAAGAACCCATCCC
	Rev	GGGATGGGTTCTTGATGTCCTGGTCCTCCT
E111R	For	CAAAAGGAGGACCAGGACATAGAGAACCCATCCCCATGT
	Rev	ACATGGGGATGGGTTCTCTATGTCCTGGTCCTCCTTTTG

[a] Mutations generated using QuikChange II XL SDM kit.
[b] For, forward; Rev, reverse.

(B) Primers used to generate G2 mutations at 5' UTR of pACYC-NGC FL plasmid

Mutation(s)[a]	Primer	
	Orientation[b]	**Sequence**
G2A	For	TTCTGCGGCCGCTAATACGACTCACTATAGAATTGTTAGTCTAC
	Rev	GCTGAAGCTAGCTTTGAAGGGGATTC
G2U	For	TTCTGCGGCCGCTAATACGACTCACTATAGATTTGTTAGTCTAC
	Rev	GCTGAAGCTAGCTTTGAAGGGGATTC
G2C	For	TTCTGCGGCCGCTAATACGACTCACTATAGACTTGTTAGTCTAC
	Rev	GCTGAAGCTAGCTTTGAAGGGGATTC

[a] Mutations generated using Phusion PCR reaction.
[b] For, forward; Rev, reverse.

(C) Primers used for site-directed mutagenesis (SDM) of pGEX-4T-1+D4(MY22713)+SAM272 plasmid

Mutation(s)[a]	Primer	
	Orientation[b]	**Sequence**
R38A	For	AAGTGGAATACTAGAAGTGGATGCAACTGAAGCCAAGTCTGCCCT
	Rev	AGGGCAGACTTGGCTTCAGTTGCATCCACTTCTAGTATTCCACTT
K42A	For	GAAGTGGATAGGACTGAAGCCGCATCTGCCCTAAGAGATGGATCT
	Rev	AGATCCATCTCTTAGGGCAGATGCGGCTTCAGTCCTATCCACTTC
R57A	For	ATCAAGCATGCGGTGTCCGCAGGGTCTAGTAAGATCAG
	Rev	CTGATCTTACTAGACCCTGCGGACACCGCATGCTTGAT
R84A	For	CGTGGATCTTGGTTGTGGGGCAGGAGGATGGTCCTATTACA
	Rev	TGTAATAGGACCATCCTCCTGCCCCACAACCAAGATCCACG
E111A	For	GGAGGTCCAGGACATGCAGAACCAATCCCCATG
	Rev	CATGGGGATTGGTTCTGCATGTCCTGGACCTCC
E111Q	For	AAGGAGGTCCAGGACATCAAGAACCAATCCCC
	Rev	GGGGATTGGTTCTTGATGTCCTGGACCTCCTT
E111R	For	CAAAAGGAGGTCCAGGACATAGAGAACCAATCCCCATGG
	Rev	CCATGGGGATTGGTTCTCTATGTCCTGGACCTCCTTTTG
R212A	For	CTCGTCAGATGCCCGCTATCCGCAAATTCTACTCATGAGATGTAT

	Rev	ATACATCTCATGAGTAGAATTTGCGGATAGCGGGCATCTGACGAG
S214A	For	CAGATGCCCGCTATCCAGGAATGCAACTCATGAGATGTATTG
	Rev	CAATACATCTCATGAGTTGCATTCCTGGATAGCGGGCATCTG
T215A	For	CCCGCTATCCAGGAATTCTGCACATGAGATGTATTGGGTGT
	Rev	ACACCCAATACATCTCATGTGCAGAATTCCTGGATAGCGGG

[a] Mutations generated using QuikChange II XL SDM kit.
[b] For, forward; Rev, reverse.

(D) Primers used to generate G2 mutations at 5' UTR of DEN4 5'UTR nt-110 DNA

Mutation(s)[a]	Primer	
	Orientation[b]	**Sequence**
G2A	For	GCGGCCGCTAATACGACTCACTATTAATTGTTAGTCTGTGTGGAC
	Rev	TGGTTCATTTTTCCAGAGATCTGC
G2U	For	GCGGCCGCTAATACGACTCACTATTATTTGTTAGTCTGTGTGGAC
	Rev	TGGTTCATTTTTCCAGAGATCTGC
G2C	For	GCGGCCGCTAATACGACTCACTATTACTTGTTAGTCTGTGTGGAC
	Rev	TGGTTCATTTTTCCAGAGATCTGC

[a] Mutations generated using Phusion PCR reaction.
[b] For, forward; Rev, reverse

References

1. Xie X, Gayen S, Kang C, Yuan Z, & Shi PY (2013) Membrane topology and function of dengue virus NS2A protein. *Journal of virology* 87(8):4609-4622.
2. Lim SP, *et al.* (2013) A crystal structure of the dengue virus non-structural protein 5 (NS5) polymerase delineates interdomain amino acid residues that enhance its thermostability and de novo initiation activities. *J Biol Chem* 288(43):31105-31114.
3. Chung KY, *et al.* (2010) Higher catalytic efficiency of N-7-methylation is responsible for processive N-7 and 2'-O methyltransferase activity in dengue virus. *Virology* 402(1):52-60.
4. Lim SP, *et al.* (2008) A scintillation proximity assay for dengue virus NS5 2'-O-methyltransferase-kinetic and inhibition analyses. *Antiviral Res* 80(3):360-369.
5. Hung M, Gibbs CS, & Tsiang M (2002) Biochemical characterization of rhinovirus RNA-dependent RNA polymerase. *Antiviral Res* 56(2):99-114.
6. Zhao Y, *et al.* (2015) A crystal structure of the Dengue virus NS5 protein reveals a novel inter-domain interface essential for protein flexibility and virus replication. *PLoS pathogens* 11(3):e1004682.
7. CCP4 (1994) The CCP4 suite: programs for protein crystallography. *Acta Crystallogr D Biol Crystallogr* 50(Pt 5):760-763.
8. Matthews BW (1968) Solvent content of protein crystals. *J Mol Biol* 33(2):491-497.
9. Collaborative Computational Project N (1994) The CCP4 suite: programs for protein crystallography. *Acta crystallographica. Section D, Biological crystallography* 50(Pt 5):760-763.
10. Adams PD, *et al.* (2010) PHENIX: a comprehensive Python-based system for macromolecular structure solution. *Acta Crystallogr D Biol Crystallogr* 66(Pt 2):213-221.
11. Emsley P & Cowtan K (2004) Coot: model-building tools for molecular graphics. *Acta Crystallogr D Biol Crystallogr* 60(Pt 12 Pt 1):2126-2132.
12. Chen VB, *et al.* (2010) MolProbity: all-atom structure validation for macromolecular crystallography. *Acta Crystallogr D Biol Crystallogr* 66(Pt 1):12-21.
13. Schrödinger L (2010) *The PyMOL Molecular Graphics System, Version 1.5.0.4*
14. Schmidt T, Schwede T, & Meuwly M (2014) Computational analysis of methyl transfer reactions in dengue virus methyltransferase. *The journal of physical chemistry. B* 118(22):5882-5890.
15. Li C, Xia Y, Gao X, & Gershon PD (2004) Mechanism of RNA 2'-O-methylation: evidence that the catalytic lysine acts to steer rather than deprotonate the target nucleophile. *Biochemistry* 43(19):5680-5687.
16. Yap LJ, *et al.* (2010) Crystal structure of the dengue virus methyltransferase bound to a 5'-capped octameric RNA. *PLoS One* 5(9).
17. Holm L & Rosenstrom P (2010) Dali server: conservation mapping in 3D. *Nucleic acids research* 38(Web Server issue):W545-549.